Frequency-renormalized multipolaron expansion for the quantum Rabi model

Lei Cong,[1] Xi-Mei Sun,[1] Maoxin Liu,[2] Zu-Jian Ying,[2,3,*] and Hong-Gang Luo[1,2,†]

[1]*Center for Interdisciplinary Studies and Key Laboratory for Magnetism and Magnetic Materials of the MoE, Lanzhou University, Lanzhou 730000, China*

[2]*Beijing Computational Science Research Center, Beijing 100084, China*

[3]*CNR-SPIN, I-84084 Fisciano (Salerno), Italy and Dipartimento di Fisica "E. R. Caianiello," Università di Salerno, I-84084 Fisciano (Salerno), Italy*

(Received 1 March 2017; published 1 June 2017)

We present a frequency-renormalized multipolaron expansion method to explore the ground state of the quantum Rabi model (QRM). The main idea is to take polaron as starting point to expand the ground state of QRM. The polarons are deformed and displaced oscillator states with variationally determined frequency-renormalization and displacement parameters. This method is an extension of the previously proposed polaron concept and the coherent state expansion used in the literature, which shows high efficiency in describing the physics of the QRM. The proposed method is expected to be useful for solving other more complicated light-matter interaction models.

DOI: 10.1103/PhysRevA.95.063803

I. INTRODUCTION

The quantum Rabi model (QRM) describes a two-level system interacting with a single-mode bosonic field [1,2]. It plays a fundamental role in many fields of physics, such as superconducting circuit quantum electrodynamics (QED) [3–5], quantum optics [6,7], quantum information [8–10], quantum computation [11], and condensed matter physics [12].

Experimentally, the model has been first realized in the cavity QED systems [13], in which the coupling strength is quite weak, corresponding to the so-called weak coupling regime. In this regime, the rotating-wave approximation (RWA) has been widely employed, which leads to an analytically solvable model, namely, the Jaynes-Cummings (JC) model [14]. The JC model is a basic model in quantum optics which is successful in understanding a range of experimental phenomena, such as the well-known quantum Rabi oscillation [15] and vacuum Rabi mode splitting [16].

Recently, with the advancement of quantum technology [17,18], the so-called strong coupling [4], ultrastrong coupling [3,19–21], and even the deep strong coupling [22] regimes have been experimentally realized in many devices. As a result, the RWA widely used in the literature is no longer valid in these strongly coupling regimes, and thus a full QRM has to be reconsidered in order to describe well the physics observed in these strongly coupling regimes.

It turns out that, despite its simple form, it is not an easy task to fully solve and understand the QRM. Therefore, many approximate methods including adiabatic approximation [23], general rotating-wave approximation (GRWA) [24] and its extensions [25–27], unitary transformation [28], and the variational technique [29], to name just a few, have been proposed. However, it has been shown that each of these approximate methods may be valid in certain limited regime, and an approximate method which is valid in whole parameter regime of the model is still favorable and deserves efforts to develop and improve. In 2011, a remarkable mathematical progress on the integrability of the QRM has been obtained by Braak [30] and thus the exact spectra of the QRM have been determined in an analytical way. The exact spectra of the QRM has also been formulated by using Bogoliubov operator technique [31]. However, in order to explore the full physics of the QRM, it is obviously not enough to only know the spectra of the model; one still needs to know exactly the wave function of the model. Therefore, it is still important to explore a simple and straightforward method to study the QRM. On the one hand, this method should be valid in the whole parameter regime of the QRM; on the other hand, it should also be convenient to formulate the wave function of the QRM. This is our motivation of the present work.

Very recently, we have introduced a trial wave function based on the concept of polaron and antipolaron picture in order to explore the phase diagram of the QRM [32]. An important feature of this trial wave function is that it provides a unified framework to accurately describe the physics of the QRM both in the weak and strong coupling regimes. However, in the crossover regime, some errors relatively are still not negligible, particularly at a low oscillator frequency, as shown in Fig. 1. Therefore, some improvements are still desirable in order to capture more accurate physics in the crossover regime.

How to further improve the calculation accuracy in the crossover regime, particularly, in the low oscillator frequency case? One notes that a variational coherent-state expansion method has been proposed by Bera *et al.* [33,34] in the study of the spin-boson model. It was shown that as more polarons are used, the result becomes more accurate. Following the idea of the multipolaron expansion, here we propose a variational *frequency-renormalized multipolaron expansion* method to improve the performance of the trial wave function based on the polaron and antipolaron picture. The key difference is that in contrast to Bera *et al.*'s multipolaron expansion, we introduce the frequency renormalization feature. As shown later, the frequency renormalization introduced shows a high efficiency in calculating the energy and wave function of the QRM. Therefore, it is expected that our frequency-renormalized

*zjying@csrc.ac.cn
†luohg@lzu.edu.cn

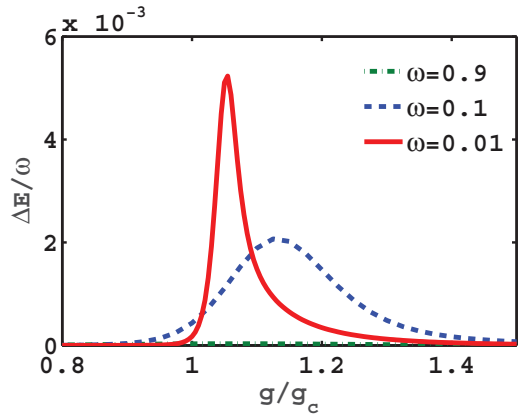

FIG. 1. Discrepancy of the ground-state energy obtained by the polaron and antipolaron trial wave function $E_{\rm gs}$ [32] in comparison to the exact diagonalization (ED) results $E_{\rm ED}$, which is given by $\Delta E/\omega = (E_{\rm gs} - E_{\rm ED})/\omega$. Here $g_c = \sqrt{\omega^2 + \sqrt{\omega^4 + g_{c_0}^4}}$ [32] and $g_{c_0} = \sqrt{\omega\Omega}/2$.

multipolaron expansion method is useful in solving more complicated models related to light-matter interaction.

The paper is organized as follows. In Sec. II, the QRM is introduced. In Sec. III, we construct our variational method based on the frequency-renormalized multipolaron expansion as the trial ground-state wave function. In Sec. IV, we present the results based on the proposed method, and compare them with those obtained by the multipolaron expansion without introducing frequency-renormalized feature. Section V is devoted to a brief conclusion.

II. THE QRM MODEL

Following the notation in Refs. [8,25,35–38], the Hamiltonian of the QRM model reads ($\hbar = m = 1$)

$$H = \frac{\Omega}{2}\sigma_x + \omega\hat{a}^\dagger\hat{a} + g\sigma_z(\hat{a}^\dagger + \hat{a}), \tag{1}$$

where Ω is the qubit energy level splitting, $\sigma_{x,z}$ is the Pauli matrix to describe the qubit, $\hat{a}^\dagger$ and $\hat{a}$ are the bosonic creation and annihilation operators, respectively, of the bosonic mode with frequency ω, and g denotes the coupling strength between the qubit and the bosonic mode.

In terms of the quantum harmonic oscillator with dimensionless formalism $\hat{a}^\dagger = (\hat{x} - i\hat{p})/\sqrt{2}$, $\hat{a} = (\hat{x} + i\hat{p})/\sqrt{2}$, where $\hat{x} = x$ and $\hat{p} = -i\frac{\partial}{\partial x}$ are the position and momentum operators respectively, the model can be rewritten as [36]

$$H = \sum_{S_z=\pm}\left(h^{S_z}|S_z\rangle\langle S_z| + \frac{\Omega}{2}|S_z\rangle\langle\bar{S}_z|\right) + \varepsilon_0, \tag{2}$$

where $+(-)$ labels the up (down) level, corresponding to the spin up (down) in the z direction, $\bar{S}_z = -S_z$.$h^\pm = \omega(\hat{p}^2 + v_\pm)/2$, with $v_\pm = (\hat{x} \pm g')^2$ which defines the bare potential, $\varepsilon_0 = -\omega(g'^2 + 1)/2$ is a constant, and $g' = \sqrt{2}g/\omega$. For simplicity, we take $\Omega = 1$ as the units of energy here and hereafter.

III. FREQUENCY-RENORMALIZED MULTIPOLARON EXPANSION METHOD

Consider the parity operator $\Pi = \sigma_x e^{i\pi a^\dagger a}$; one has $[H,\Pi]=0$. Such a $\mathbb{Z}_2$ symmetry leads to a decomposition of the state space into just two subspaces with odd and even parity, respectively. Since the ground state has an odd parity, one takes the trial wave function of the QRM in the position representation as

$$|G\rangle = \frac{1}{\sqrt{2}}(\Psi^+(x)|+_z\rangle - \Psi^-(x)|-_z\rangle), \tag{3}$$

where $\Psi^\pm$ is the wave function associated with the spin state $|\pm_z\rangle$, and we have

$$\Psi^+(x) = \Psi^-(-x). \tag{4}$$

With the ground-state wave function $|G\rangle$, the Schrödinger equation becomes $\frac{1}{2}\omega(\hat{p}^2 + v_\pm + \delta v_\pm)\Psi^\pm = E\Psi^\pm$, where $\delta v_\pm = -\frac{\Omega}{\omega}\frac{\Psi^\mp}{\Psi^\pm}$ is an additional potential induced by the tunneling between two levels, and E is the ground-state energy. The additional potential will deform the bare potential and most importantly it will create a subwell in the opposite direction of the bare potential $v_\pm$. As a result, such an effective potential exhibits a double-well structure for appropriate parameter regimes [32,39]. Based on the polaron picture [32–34], the wave functions $\Psi^\pm$ are expanded as

$$\Psi^\pm(x) = \sum_{n=1}^{N} C_n\varphi_n^\pm(x), \tag{5}$$

where C_n is the coefficient and N is the number of polaron used. Here $\varphi_n^\pm(x) = \phi_0(\xi_n\omega, x \pm \zeta_n g')$ denotes the nth polaron which is given by deforming oscillator ground-state wave function $\phi_0(\omega,x)$ with the frequency renormalization parameter ξ_n and shifted position parameter ζ_n. As a result, one obtains $\varphi_n^\pm(x) = (\frac{\xi_n}{\pi})^{\frac{1}{4}}e^{-\frac{(x\pm\zeta_n g')^2\xi_n}{2}}$.

Thus, Eq. (3) can be rewritten as

$$|G\rangle = \frac{1}{\sqrt{2}}\sum_{n=1}^{N} C_n(\phi_0(\xi_n\omega, x + \zeta_n g')|+_z\rangle - \phi_0(\xi_n\omega, x - \zeta_n g')|-_z\rangle), \tag{6}$$

which is the starting point of the present work. Due to the deformed polaron introduced, we call Eq. (6) as frequency-renormalized multipolaron expansion (FR-MPE). Actually, if one takes $N = 2$, Eq. (6) recovers the previous polaron and antipolaron wave function which has been used to explore the ground-state phase diagram of the Rabi model [32]. On the other hand, if one takes $\xi_n = 1$, i.e., the frequency-renormalization factor is not considered, Eq. (6) is the single-mode version of the coherent state expansion used in the study of the spin-boson model [33,34], since a coherent state is a displaced oscillator state in the $\hat{x}$ representation.

The variational parameters introduced in Eq. (6), i.e., C_n, ξ_n and ζ_n ($n = 1,\ldots,N$), can be determined by minimizing the ground-state energy $E_G = \langle G|H|G\rangle$ (see the appendix for a detailed derivation), subject to the constraint of wave-function normalization $\langle G|G\rangle = 1$, under which the number of variational parameters will be $3\times N - 1$. In order to determine the variational parameters, we first adopt simulated annealing

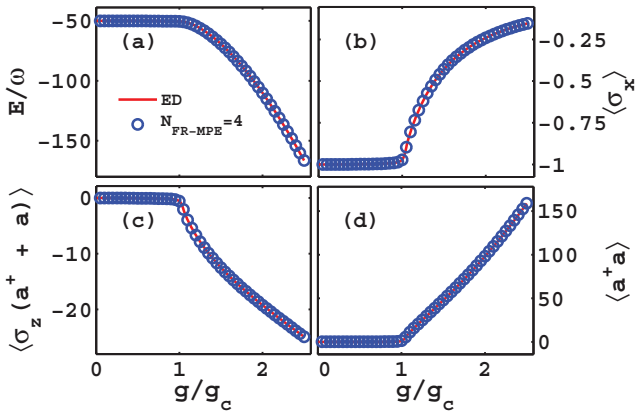

FIG. 2. Ground-state physical quantities as functions of the coupling strength g/g_c. (a) The ground-state energy. (b) The spin polarization $\langle\sigma_x\rangle$. (c) The correlation function $\langle\sigma_z(a^+ + a)\rangle$. (d) The mean photon number $\langle a^+a\rangle$. The red lines are the exact diagonalization results taken as benchmarks, and the blue circles are our results obtained by our frequency-renormalized multipolaron expansion given by Eq. (6). Here we take $\omega = 0.01$ and $N = 4$.

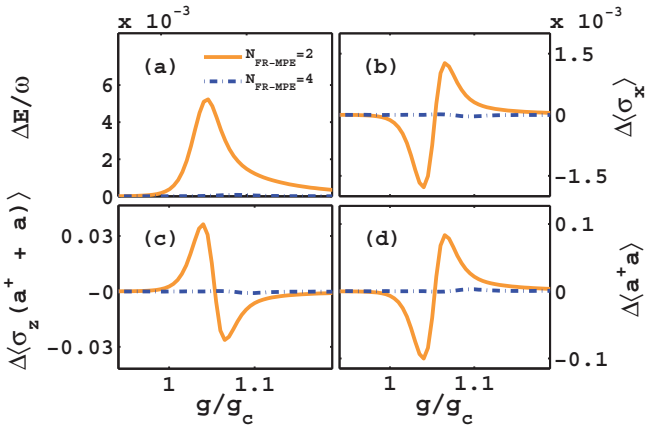

FIG. 3. Comparison of errors of various physical quantities between $N = 4$ and $N = 2$. The yellow lines are the result of $N = 2$ and the dash-dotted lines represent the result of $N = 4$. (a) Error in the ground-state energy with respect to the ED result $\Delta E/\omega = (E - E_{\rm ED})/\omega$. (b) Error in the tunneling strength $\Delta\langle\sigma_x\rangle = \langle\sigma_x\rangle - \langle\sigma_x\rangle_{\rm ED}$. (c) Error in the correlation function $\Delta\langle\sigma_z(a^+ + a)\rangle = \langle\sigma_z(a^+ + a)\rangle - \langle\sigma_z(a^+ + a)\rangle_{\rm ED}$. (d) Error in the mean photon number $\Delta\langle a^+a\rangle = \langle a^+a\rangle - \langle a^+a\rangle_{\rm ED}$. Here we take $\omega = 0.01$.

algorithm [40,41] to search the rough values of the variational parameters. Then we use pattern search algorithm [42,43] to refine these variational parameter values in order to further minimize the ground-state energy. The combination of these two algorithms is found to be sufficient to determine the variational parameters with high efficiency and high precision.

IV. NUMERICAL RESULTS AND DISCUSSION

A. The result with $N = 4$

First of all, we present some results to show the high precision of our method. As shown in Fig. 1, as the oscillator frequency is lower, the error near g_c is larger. Moreover, the main error is located around g_c. Here $g_c = \sqrt{\omega^2 + \sqrt{\omega^4 + g_{c0}^4}}$, denoting a coupling strength separating the quadpolaron and bipolaron regimes [32] for finite oscillator frequency. In the low-frequency limit, namely, $\omega/\Omega \to 0$, g_c approaches g_{c0}, a commonly used value in the literature [8,44]. Therefore, here we consider the case of $\omega = 0.01$ and take $N = 4$. Meanwhile, we compare the obtained results with those with numerical exact diagonalization. In Fig. 2 we show various physical quantities including (a) the ground-state energy, (b) the spin polarization $\langle\sigma_x\rangle$, (c) the correlation $\langle\sigma_z(a^\dagger + a)\rangle$, and (d) the mean photon number $\langle a^\dagger a\rangle$ as a function of the coupling strength. Due to the aforementioned reason, hereafter we limit ourself to the region around g_c. It is found that the agreement is quite good, which will be further discussed in the next subsection. This result confirms the high precision of our method, even in the low-oscillator-frequency regime. In addition, our method also exhibits high efficiency since only two pairs of polaron and antipolaron ($N = 4$) have been considered here, which indicates that the deformed polaron picture [32] is a good starting point to capture the physics of the QRM.

B. The high efficiency of the frequency-renormalized multipolaron expansion

In order to confirm the high efficiency of the frequency-renormalized multipolaron expansion method, we compare the result with $N = 4$ with that of $N = 2$ with $\omega = 0.01$ in Fig. 3. As also mentioned above, the case of $N = 2$ recovers the previous polaron and antipolaron picture [32]. From Fig. 3 it is noted that the results for $N = 4$ have a vanishingly small error in comparison to that of $N = 2$. Technically, we just increase an additional pair of polaron and antipolaron beyond that of $N = 2$, leading to a dramatic improvement, which shows the high efficiency of the polaron and antipolaron basis. Physically, it is not difficult to understand why the polaron and antipolaron basis is so high efficient. This is because the polaron and antipolaron, as basic ingredients in describing the ground-state wave function of the QRM, are able to capture the essential physics of the model. The antipolaron component originates naturally from the tunneling feature [32,36] of the QRM. By the same reason, the additional pair of polaron and antipolaron also originate from the high-order effect of the tunneling feature. This point is more clear in the discussion of the ground-state wave function below.

Figure 4 shows the ground-state wave function of the QRM for $N = 4$ and its polaron components. As a comparison, we also present the result for $N = 2$. For simplicity, we only provide the Ψ^+ component, and the Ψ^- has a similar behavior due to the odd parity. From Fig. 4(a), although the case of $N = 2$ captures the nature of the wave-packet separation for $g/g_c = 1.05$, the error from the numerical exact result is still obvious, as shown in Fig. 4(c) as yellow dashed line. In particular, in the region around $x = 0$, the error is more obvious. This is because that after the wave packet becomes separated, a pair of polaron and antipolaron is not sufficient to describe the region away from the positions of the polaron and antipolaron, for example, the region of $x = 0$. Therefore, according to the

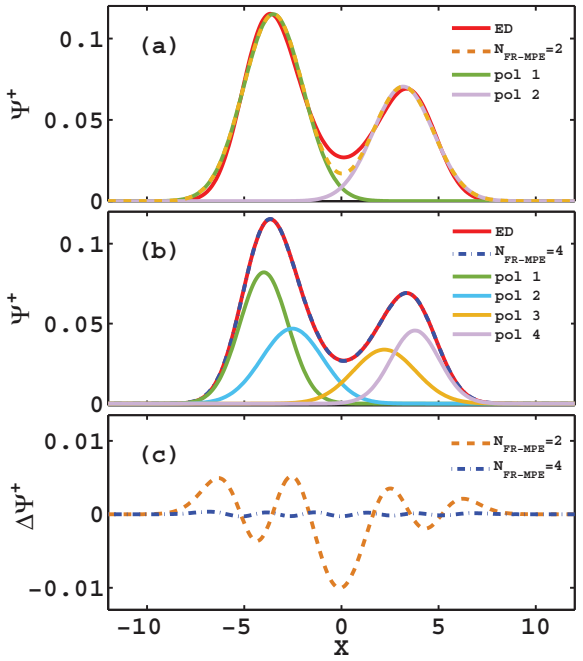

FIG. 4. Comparison of ground-state wave function Ψ^+ for the $|+\rangle$ component obtained by the frequency-renormalized multipolaron expansion with $N = 2$ and $N = 4$. The numerical exact result is taken as the benchmark. (a) $N_{\mathrm{FR-MPE}} = 2$. (b) $N_{\mathrm{FR-MPE}} = 4$. (c) Error of Ψ^+ in comparison to the numerical exact one. $\Delta\Psi^+ = \Psi^+_{\mathrm{FR-MPE}} - \Psi^+_{\mathrm{ED}}$. The other parameters are $g/g_c = 1.05$ and $\omega = 0.01$.

idea of the frequency-renormalized multipolaron expansion, one increases an additional pair of polaron and antipolaron, and not only the region away from the positions of the polaron and antipolaron but the whole wave function has a vanishing small error in comparison with the exact one, as shown in Fig. 4(c) by the blue dash-dotted line. This result indicates that the frequency-renormalized multipolaron expansion is highly efficient in calculating the wave function of the QRM and as a result is able to calculate accurately the physical observables, as shown in Fig. 3.

C. The importance of the frequency renormalization

Based on the scheme of multipolaron expansion introduced by Bera *et al.* in their coherent-state expansion (CSE) method [33,34], one of the important features of our method is introduction of the frequency renormalization feature. The physical background of the introduction of the frequency renormalization is the change of the effective potentials induced by the tunneling between these two energy levels, which is the origin of the antipolaron. The existence of the effective potentials would, of course, modify the frequency of the oscillator states in the QRM. In order to show the importance of the frequency renormalization, in the following we compare our method with the frequency renormalization with the simple multipolaron expansion without the frequency renormalization. The latter is called the CSE method below, which has been used to study the spin-boson model. Here we employ it to the QRM.

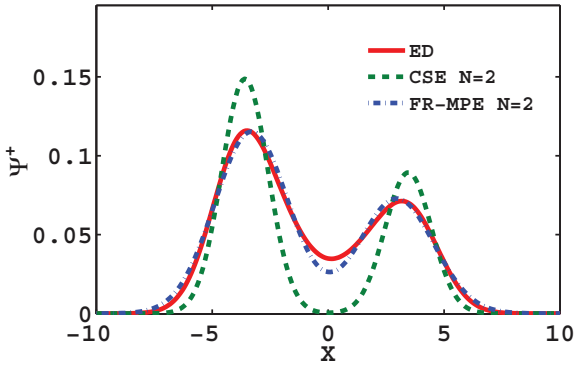

FIG. 5. Comparison of the ground-state wave functions obtained by the multipolaron expansion with and without frequency renormalization with the numerical exact result for $N = 2$. The other parameters are $g/g_c = 1.05$ and $\omega = 0.01$.

First, we consider the ground-state wave function for the Ψ^+ component obtained by these two methods, as shown in Fig. 5, and also present the numerical exact wave function for comparison. It is quite obvious that the result with the frequency renormalization agrees much better with the exact one than that without the frequency renormalization. The

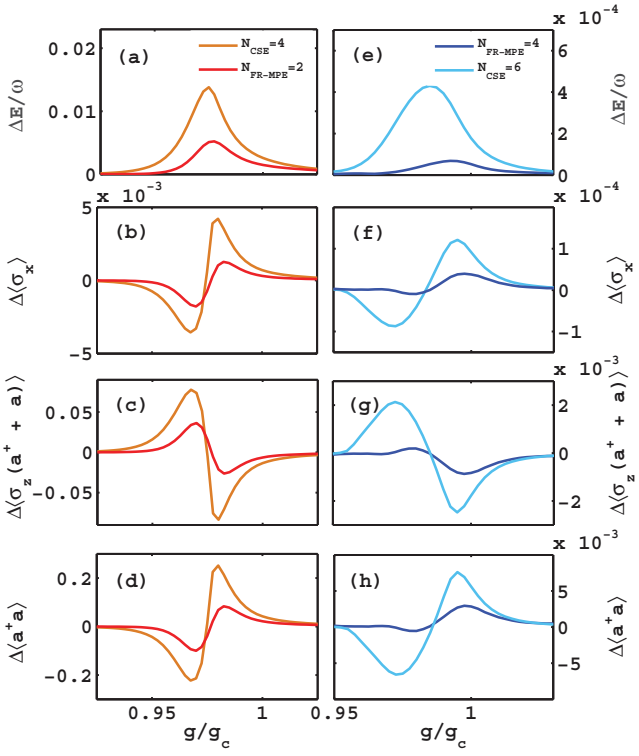

FIG. 6. Comparison of the ground-state energy and the other physical observables obtained by the multipolaron expansion method with and without frequency renormalization. Left column: comparison between $N_{\mathrm{FR-MPE}} = 2$ and $N_{\mathrm{CSE}} = 4$. Right column: comparison between $N_{\mathrm{FR-MPE}} = 4$ and $N_{\mathrm{CSE}} = 6$. For the left column, the variational parameters for our scheme is 5 and that of the CSE used is 7. In the right column, the variational parameters used are the same; both are 11. The errors are defined the same as those in Fig. 3.

comparison indicates that the frequency renormalization is indeed an important feature in describing the ground-state physics of the QRM. This feature is even more important than simply increasing the number of the polaron and antipolaron. This can be clearly seen from Fig. 6, showing the comparison of the ground-state energy and the other physical observables between the results with frequency renormalization for $N_{\mathrm{FR-MPE}} = 2,4$ and without frequency renormalization for $N_{\mathrm{CSE}} = 4,6$, respectively. Obviously, our method has much higher efficiency than that without the frequency renormalization. Moreover, the corresponding variational parameters in our scheme are less than or equal to those of the CSE.

V. CONCLUSIONS

Based on the polaron and antipolaron picture, we proposed a frequency renormalization multipolaron expansion method to improve significantly the ground-state wave function of QRM, as a result, the ground-state energy and other physical quantities have also been significantly improved, in particular, near the crossover region. In comparison to the coherent state expansion given by Bera *et al.* [33,34], our method shows higher efficiency, in which the frequency renormalization plays an important role. Physical origin of the frequency renormalization is due to the additional potential induced by the tunneling between two energy levels. This method can be applied to other more complicated quantum models like the spin-boson model [33,34], multiqubit QRM [45,46], anisotropic QRM [47], and biased or asymmetric Rabi model [48], and so on. Further works are in progress.

ACKNOWLEDGMENTS

We acknowledges useful discussion with Gao-Yang Li, Fu-Zhou Chen, Chong Chen, and Chen Cheng. This work was supported by NSFC (Grants No. 11325417 and No. 11674139) and PCSIRT (Grant No. IRT-16R35). Z.-J.Y. also acknowledges the financial support of the Future and Emerging Technologies (FET) programme within the Seventh Framework Programme for Research of the European Commission, under FET-Open Grant No. 618083 (CNTQC).

APPENDIX: THE GROUND STATE ENERGY OF FR-MPE

In this appendix, we present the main steps to get the ground-state energy. The ground state $|G\rangle$ of FR-MPE is

$$|G\rangle = \frac{1}{\sqrt{2}}\sum_{n=1}^{N} C_n(\varphi_n^+|+_z\rangle - \varphi_n^-|-_z\rangle). \tag{A1}$$

The ground-state energy of FR-MPE is given by

$$\begin{aligned} E_{\mathrm{FR-MPE}} &= \langle G|H|G\rangle \\ &= \frac{1}{2}\sum_{n,m}^{N} C_nC_m\Big[(\langle\varphi_n^+|h^+|\varphi_m^+\rangle + \langle\varphi_n^-|h^-|\varphi_m^-\rangle) \\ &\quad - \frac{\Omega}{2}(\langle\varphi_n^+|\varphi_m^-\rangle + \langle\varphi_n^-|\varphi_m^+\rangle)\Big] - \frac{1}{2}\omega(g'^2+1) \\ &= \sum_{n,m}^{N} C_nC_m\langle\varphi_n^+|h^+|\varphi_m^+\rangle - \frac{\Omega}{2}\sum_{n,m}^{N}\langle\varphi_n^+|\varphi_m^-\rangle \\ &\quad - \frac{1}{2}\omega(g'^2+1). \end{aligned} \tag{A2}$$

1. Calculation of each term

For the first term in Eq. (A2)

$$\begin{aligned} h_{nm}^+ &= \langle\varphi_n^+|h^+|\varphi_m^+\rangle \\ &= \frac{1}{2}\omega\langle\varphi_n^+|[\hat{p}^2 + (\hat{x}+g')^2]|\varphi_m^+\rangle \\ &= \frac{1}{2}\omega\langle\varphi_n^+|\left(-\frac{\partial^2}{\partial x^2} + x^2 + 2xg' + g'^2\right)|\varphi_m^+\rangle. \end{aligned} \tag{A3}$$

For simplicity, we have assumed the unit $\hbar = m = 1$.

We first give the first term in Eq. (A3):

$$\begin{aligned} \langle\varphi_n^+|\left(-\frac{\partial^2}{\partial x^2}\right)|\varphi_m^+\rangle &= -\langle\varphi_n^+|(4D^2x^2 + 4DEx \\ &\quad + E^2 + 2D)|\varphi_m^+\rangle, \end{aligned} \tag{A4}$$

where the coefficients D and E are introduced for the simplicity of the formulation; they are defined as

$$D = -\tfrac{1}{2}\xi_m; \quad E = -g'\xi_m\zeta_m. \tag{A5}$$

So, the expression of Eq. (A3) is

$$\begin{aligned} h_{nm}^+ &= \tfrac{1}{2}\omega\langle\varphi_n^+|[(1-4D^2)x^2 + (2g' - 4DE)x \\ &\quad - E^2 - 2D + g'^2]|\varphi_m^+\rangle, \end{aligned} \tag{A6}$$

in which

$$\begin{aligned} S_{nm} &= \langle\varphi_n^+(x)|\varphi_m^+(x)\rangle \\ &= \sqrt{2}\left[\frac{\xi_n\xi_m}{(\xi_n+\xi_m)^2}\right]^{\frac{1}{4}} e^{\left(-\frac{(\zeta_n-\zeta_m)^2g'^2\xi_n\xi_m}{2(\xi_n+\xi_m)}\right)}, \end{aligned} \tag{A7}$$

$$\begin{aligned} \langle\hat{x}\rangle_{nm} &= \langle\varphi_n^+(x)|\hat{x}|\varphi_m^+(x)\rangle \\ &= S_{nm}\frac{-\xi_m\zeta_m - \xi_n\zeta_n}{\xi_n+\xi_m}g', \end{aligned} \tag{A8}$$

and

$$\begin{aligned} \langle\hat{x}^2\rangle_{nm} &= \langle\varphi_n^+|\hat{x}^2|\varphi_m^+\rangle \\ &= S_{nm}\left\{\frac{1}{\xi_n+\xi_m} + \left[\frac{(\xi_m\zeta_m + \xi_n\zeta_n)g'}{\xi_n+\xi_m}\right]^2\right\}. \end{aligned} \tag{A9}$$

Now, we can get the first term in Eq. (A2) completely.

For the second term in Eq. (A2),

$$\begin{aligned} S_{n\bar{m}} &= \langle\varphi_n^+|\varphi_m^-\rangle = \langle\varphi_n^+(x)|\varphi_m^+(-x)\rangle \\ &= \sqrt{2}\left[\frac{\xi_n\xi_m}{(\xi_n+\xi_m)^2}\right]^{\frac{1}{4}} e^{\left(-\frac{(\zeta_n+\zeta_m)^2g'^2\xi_n\xi_m}{2(\xi_n+\xi_m)}\right)}, \end{aligned} \tag{A10}$$

so we finally can get the ground-state energy.

2. Normalization condition

Besides the above formulation, we still have the normalization condition which describes the relationships between the

parameters:

$$\langle G|H|G\rangle = \frac{1}{2}\sum_{n,m}^{N} C_n C_m(\langle\varphi_n^+|\varphi_m^+\rangle + \langle\varphi_n^-|\varphi_m^-\rangle)$$
$$= \sum_{n,m}^{N} C_n C_m(\langle\varphi_n^+|\varphi_m^+\rangle) = 1. \quad \text{(A11)}$$

The derivations of the ground-state energies of CSE and FR-MPE are nearly the same, since in the $\hat{x}$ representation, a coherent state is a displaced ground state of the oscillator. We can get the CSE result by simply setting frequency renormalization factor $\xi = 1$ in FR-MPE. So here we present the derivation of FR-MPE result only.

[1] I. I. Rabi, Phys. Rev. **49**, 324 (1936).
[2] I. I. Rabi, Phys. Rev. **51**, 652 (1937).
[3] T. Niemczyk, F. Deppe, H. Huebl, E. P. Menzel, F. Hocke, M. J. Schwarz, J. J. Garcia-Ripoll, D. Zueco, T. Hummer, E. Solano, A. Marx, and R. Gross, Nat. Phys. **6**, 772 (2010).
[4] A. Wallraff, D. I. Schuster, A. Blais, L. Frunzio, R. S. Huang, J. Majer, S. Kumar, S. M. Girvin, and R. J. Schoelkopf, Nature (London) **431**, 162 (2004).
[5] A. Wallraff, D. I. Schuster, A. Blais, L. Frunzio, J. Majer, M. H. Devoret, S. M. Girvin, and R. J. Schoelkopf, Phys. Rev. Lett. **95**, 060501 (2005).
[6] J. M. Raimond, M. Brune, and S. Haroche, Rev. Mod. Phys. **73**, 565 (2001).
[7] M. O. Scully and M. S. Zubairy, *Quantum Optics* (Cambridge University Press, Cambridge, UK, 1997).
[8] S. Ashhab and F. Nori, Phys. Rev. A **81**, 042311 (2010).
[9] Z. Zhou, Z. Lü, and H. Zheng, Quantum Inf. Proc. **15**, 3223 (2016).
[10] Y.-J. Zhao, C. Wang, X. Zhu, and Y.-x. Liu, Sci. Rep. **6**, 23646 (2016).
[11] G. Romero, D. Ballester, Y. M. Wang, V. Scarani, and E. Solano, Phys. Rev. Lett. **108**, 120501 (2012).
[12] T. Holstein, Ann. Phys. **8**, 325 (1959).
[13] Z.-L. Xiang, S. Ashhab, J. Q. You, and F. Nori, Rev. Mod. Phys. **85**, 623 (2013).
[14] E. T. Jaynes and F. W. Cummings, Proc. IEEE **51**, 89 (1963).
[15] M. Brune, F. Schmidt-Kaler, A. Maali, J. Dreyer, E. Hagley, J. M. Raimond, and S. Haroche, Phys. Rev. Lett. **76**, 1800 (1996).
[16] R. J. Thompson, G. Rempe, and H. J. Kimble, Phys. Rev. Lett. **68**, 1132 (1992).
[17] D. Leibfried, R. Blatt, C. Monroe, and D. Wineland, Rev. Mod. Phys. **75**, 281 (2003).
[18] D. Englund, A. Faraon, I. Fushman, N. Stoltz, P. Petroff, and J. Vuckovic, Nature (London) **450**, 857 (2007).
[19] B. Peropadre, P. Forn-Díaz, E. Solano, and J. J. García-Ripoll, Phys. Rev. Lett. **105**, 023601 (2010).
[20] P. Forn-Díaz, J. Lisenfeld, D. Marcos, J. J. García-Ripoll, E. Solano, C. J. P. M. Harmans, and J. E. Mooij, Phys. Rev. Lett. **105**, 237001 (2010).
[21] C. K. Andersen and A. Blais, New J. Phys. **19**, 023022 (2017).
[22] J. Casanova, G. Romero, I. Lizuain, J. J. García-Ripoll, and E. Solano, Phys. Rev. Lett. **105**, 263603 (2010).
[23] E. K. Irish, J. Gea-Banacloche, I. Martin, and K. C. Schwab, Phys. Rev. B **72**, 195410 (2005).
[24] E. K. Irish, Phys. Rev. Lett. **99**, 173601 (2007).
[25] Y. Zhang, G. Chen, L. Yu, Q. Liang, J.-Q. Liang, and S. Jia, Phys. Rev. A **83**, 065802 (2011).
[26] Y.-Y. Zhang, Phys. Rev. A **94**, 063824 (2016).
[27] L. Yu, S. Zhu, Q. Liang, G. Chen, and S. Jia, Phys. Rev. A **86**, 015803 (2012).
[28] Y. Yan, Z. Lü, and H. Zheng, Phys. Rev. A **91**, 053834 (2015).
[29] M. Liu, Z.-J. Ying, J.-H. An, and H.-G. Luo, New J. Phys. **17**, 043001 (2015).
[30] D. Braak, Phys. Rev. Lett. **107**, 100401 (2011).
[31] Q.-H. Chen, C. Wang, S. He, T. Liu, and K.-L. Wang, Phys. Rev. A **86**, 023822 (2012).
[32] Z.-J. Ying, M. Liu, H.-G. Luo, H.-Q. Lin, and J. Q. You, Phys. Rev. A **92**, 053823 (2015).
[33] S. Bera, S. Florens, H. U. Baranger, N. Roch, A. Nazir, and A. W. Chin, Phys. Rev. B **89**, 121108 (2014).
[34] S. Bera, A. Nazir, A. W. Chin, H. U. Baranger, and S. Florens, Phys. Rev. B **90**, 075110 (2014).
[35] V. V. Albert, Phys. Rev. Lett. **108**, 180401 (2012).
[36] E. K. Irish and J. Gea-Banacloche, Phys. Rev. B **89**, 085421 (2014).
[37] Y.-Y. Zhang, Q.-H. Chen, and Y. Zhao, Phys. Rev. A **87**, 033827 (2013).
[38] T. Liu, M. Feng, W. L. Yang, J. H. Zou, L. Li, Y. X. Fan, and K. L. Wang, Phys. Rev. A **88**, 013820 (2013).
[39] M. A. Bastarrachea-Magnani, A. Relao, S. Lerma-Hernndez, B. L. del Carpio, J. Chvez-Carlos, and J. G. Hirsch, J. Phys. A **50**, 144002 (2017).
[40] S. Kirkpatrick, J. Stat. Phys. **34**, 975 (1984).
[41] P. J. M. van Laarhoven and E. H. L. Aarts, in *Simulated Annealing: Theory and Applications* (Springer, Dordrecht, 1987), pp. 7–15.
[42] R. Hooke and T. A. Jeeves, J. ACM **8**, 212 (1961).
[43] W. C. Davidon, SIAM J. Optim. **1**, 1 (1991).
[44] R. Graham and M. Höhnerbach, Z. Phys. B **57**, 233 (1984).
[45] F. Benatti, R. Floreanini, and U. Marzolino, Phys. Rev. A **81**, 012105 (2010).
[46] L. Mao, Y. Liu, and Y. Zhang, Phys. Rev. A **93**, 052305 (2016).
[47] Q.-T. Xie, S. Cui, J.-P. Cao, L. Amico, and H. Fan, Phys. Rev. X **4**, 021046 (2014).
[48] M. Liu, Z.-J. Ying, J.-H. An, H.-G. Luo, and H.-Q. Lin, J. Phys. A **50**, 084003 (2017).